First-principles study on the effect of high In doping on the conductivity of ZnO*

Hou Qing-Yu(侯清玉)[a)†], Li Ji-Jun(李继军)[a)‡], Ying Chun(迎 春)[a)], Zhao Chun-Wang(赵春旺)[a)], Zhao Er-Jun(赵二俊)[a)], and Zhang Yue(张 跃)[b)]

[a)] School of Science, Inner Mongolia University of Technology, Hohhot 010051, China
[b)] School of Material Science and Engineering, Beijing University of Aeronautics and Astronautics, Beijing 100083, China

(Received 26 July 2012; revised manuscript received 2 March 2013)

Based on the density functional theory (DFT), using first-principles plane-wave ultrasoft pseudopotential method, the models of the unit cell of pure ZnO and two highly In-doped supercells of $Zn_{0.9375}In_{0.0625}O$ and $Zn_{0.875}In_{0.125}O$ are constructed, and the geometry optimizations of the three models are carried out. The total density of states (DOS) and the band structures (BS) are also calculated. The calculation results show that in the range of high doping concentration, when the doping concentration is hihger than a specific value, the conductivity decreases with the increase of the doping concentration of In in ZnO, which is in consistence with the change trend of the experimental results.

Keywords: wurtzite ZnO, high In doping, conductivity, first principles

PACS: 71.15.–m, 74.20.Pq, 72.15.–v **DOI:** 10.1088/1674-1056/22/7/077103

1. Introduction

The demand of low cost and high performance optoelectronic devices leads to the development of more efficient transparent conductive oxide (TCO) thin films, mainly for applications such as solar cells,[1,2] liquid crystal displays, piezoelectric devices,[3] surface acoustic wave devices,[4] etc. To date, the industry standard in TCO has been indium–tin–oxide (ITO). In the recent two decades, ZnO has emerged as one of the most promising materials due to its good photoelectric properties together with its abundance in nature, which makes it a low cost material compared with the ITO. The resistivity of undoped ZnO thin film has attained to the order of 10^{-4} Ω·cm,[5] but its behavior is not stable, especially at high temperature. In order to improve the stability and photoelectric properties of ZnO thin film, the research on the doping technique of ZnO has been performed. The experimental researches on In-doped ZnO thin film have attracted much attention,[6–11] and the theoretical studies on In-doped ZnO by using first-principles have also been reported. Xie *et al.*[12] studied the optical properties of In-doped wurtzite ZnO based on first-principle. Zhou *et al.*[13] investigated the electronic energy band structure of In-doped ZnO transparent conducting oxide by density functional calculations using local density approximation + Hubbard U (LDA + U) scheme. Kim and Park[14] studied the large and abrupt optical band gap variation in In-doped ZnO based on first-principles. Li *et al.*[15] calculated the electronic structures and effective mass values of the N mono-doped and Al–N, Ga–N, In–N codoped ZnO system by first-principle method. However, there is little research about the effect of high In doping on the conductivity of ZnO based on first-principles. In this paper, we present a first-principles study on the effect of high In doping on the conductivity of ZnO. However, there are some differences in the conductivity of heavily In-doped ZnO in a range of 1 at%–2.15 at% (2.79 wt%–6 wt%). It was indicated in Ref. [16] that the larger the doping concentration, the greater the conductivity is. The results are in discrepancy with the results in Ref. [17]. Due to the periodicity of the crystal, we can only study the conductivity of ZnO doped with In by first-principles in a similar doping concentration range to those in Refs. [16] and [17], and obtain some useful results. We believe that these results would be helpful for the further preparation of In-doped ZnO in experiment.

2. Models and method

The ideal ZnO has a hexagonal wurtzite structure with a space group $P63/mc$ and $C6v$-4 symmetry. The $1 \times 1 \times 1$ unit cell of pure ZnO, $2 \times 2 \times 4$ supercell of $Zn_{0.96875}In_{0.03125}O$ with an In concentration of 1.56 at% (4.35 wt%) (Fig. 1), and the $3 \times 2 \times 2$ supercell of $Zn_{0.9583}In_{0.0417}O$ with an In concentration of 2.08 at% (5.77 wt%) (Fig. 2) are used as computational models. In $Zn_{0.96875}In_{0.03125}O$ and $Zn_{0.9583}In_{0.0417}O$, one In atom has substituted for one Zn atom. Because the doping mode is substitution doping, the $Zn_{0.96875}In_{0.03125}O$ and

*Project supported by the National Natural Science Foundation of China (Grant Nos. 51261017 and 21261013), the Ministry of Education "Spring Sunshine" Plan Funding, China, the Natural Science Foundation of Inner Mongolia Autonomous Region, China (Grant No. 2011BS0104), and the College Science Research Project of Inner Mongolia Autonomous Region, China (Grant Nos. NJZY12068 and NJZZ13099).

†Corresponding author. E-mail: by0501119@126.com
‡Corresponding author. E-mail: lijjtom@yahoo.com.cn

© 2013 Chinese Physical Society and IOP Publishing Ltd

$Zn_{0.9583}In_{0.0417}O$ are isomorphic with the pure ZnO.[18]

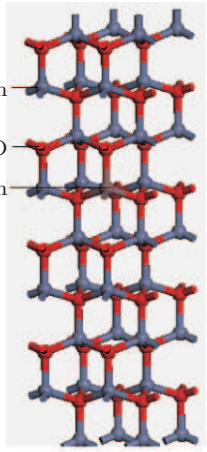


Fig. 1. (color online) The 2×2×4 supercell of $Zn_{0.96875}In_{0.03125}O$.

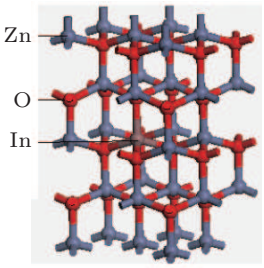


Fig. 2. (color online) The 3×2×2 supercell of $Zn_{0.9583}In_{0.0417}O$.

The calculations are based on the density functional theory (DFT) with the generalized gradient approximation (GGA) and the plane-wave pseudopotentials as implemented in the CASTEP code.[19] The GGA with the Perdew–Burke–Ernzerhof exchange–correlation functional is employed in the simulations. Ultrasoft pseudopotentials are utilized for the geometry optimization to render the computations tractable as well as to enhance efficiency. The valence atomic configurations are $3d^{10}\ 4s^2$ for Zn, $2s^2\ 2p^4$ for O, and $4d^{10}\ 5s^2\ 5p^1$ for In. In our calculation, the spin polarization effect is not considered, and the energy cutoff for the plane wave expansion is set to be 340 eV, meanwhile, the calculation precision is set to be 1.0×10^{-5} eV/atom. All atoms are allowed to relax until the force on each atom is below 0.5 eV/nm, and the internal stress is below 0.05 Gpa, at the same time the displacement of each atom is below 0.0001 nm. For the Brillouin zone integration, we use a 9×9×6 *k*-point Monkhorst–Pack mesh for the unit cell of pure ZnO, a 4×4×1 *k*-point Monkhorst–Pack mesh for the supercell of $Zn_{0.96875}In_{0.03125}O$, and a 4×3×2 *k*-point Monkhorst–Pack mesh for the supercell of $Zn_{0.9583}In_{0.0417}O$.

3. Results and discussion

3.1. Geometry optimization results

The optimized geometry parameters and total energy of $Zn_{1-x}In_xO$ ($x = 0$, 0.03125, 0.0417) are presented in Table 1. It is clear that the lattice constants and volume slightly increase with the doping concentration of In increasing, and this is because the ionic radius of In^{3+} (0.080 nm) is larger than that of Zn^{2+} (0.074 nm). It can also be seen that the total energy slightly increases with the doping concentration of In increasing, which indicates that the system stability slightly decreases due to the increase of the repelling interaction among the superfluous positive charges of In^{3+}.[20] In addition, considering the system stability, the most possible substitution locations are determined in $Zn_{0.96875}In_{0.03125}O$ and $Zn_{0.9583}In_{0.0417}O$ according to the lowest energy principle.

Table 1. Optimized geometry parameters and total energies of $Zn_{1-x}In_xO$ ($x = 0$, 0.03125, 0.0417).

Models	*a*/nm	*b*/nm	*c*/nm	V/nm^3	*E*/eV
ZnO	0.3298	0.3298	0.5318	0.0500	–4311.5
$Zn_{0.96875}In_{0.03125}O$	0.3245	0.3245	0.5386	0.05156	–4288.8
$Zn_{0.9583}In_{0.0417}O$	0.3317	0.3317	0.5355	0.05200	–4285.7

3.2. Doping concentration

When the magnitude of doping concentration is less than 10^{18} cm^{-3}, the doped semiconductor is considered to be low doping. At this time, the doping concentration has almost no effect on mobility, and so the mobility is assumed to be constant. But when the magnitude of doping concentration is equal to or greater than 10^{18} cm^{-3}, the doped semiconductor is considered to be high doping. At this time, the doping concentration has a great effect on mobility, and the mobility is variable.[21] In this paper, after geometry optimization, the doping concentration of In is 1.21×10^{21} cm^{-3} in $Zn_{0.96875}In_{0.03125}O$, and it is 1.60×10^{21} cm^{-3} in $Zn_{0.9583}In_{0.0417}O$. So, both of them belong in high doping.

3.3. Conductivity

The electron conductivity is related to the relative electron number and the electron mobility. So here we first consider the effect of high In doping on relative electron number and electron mobility, and then analyze the effect of high In doping on the conductivity of ZnO.

3.3.1. Relative electron number

Figures 3–5 show the total density of states (DOS) of the unit cell of pure ZnO, $Zn_{0.96875}In_{0.03125}O$, and $Zn_{0.9583}In_{0.0417}O$, respectively, where the valence band is represented by VB, and the conduction band is denoted by CB.

From Fig. 3, we can see that the Fermi level of the unit cell of pure ZnO is at the top of the VB. It must be point out that according to the general definition, the Fermi level of pure ZnO is near the middle of the band gap, but in the present paper the Fermi level has been specified to be 0 eV.[22]

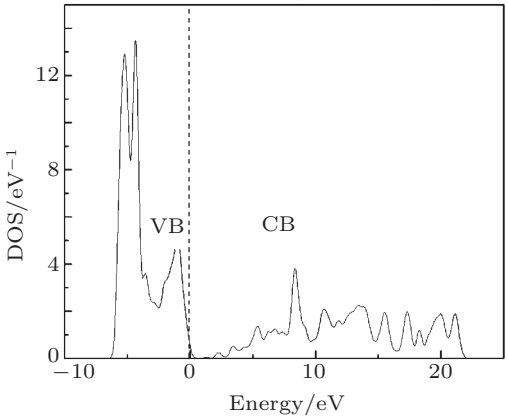


Fig. 3. Total density of states (DOS) of the unit cell of pure ZnO.

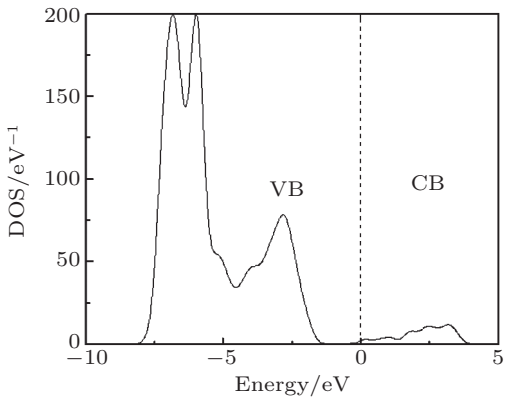


Fig. 4. Total density of states (DOS) of $Zn_{0.96875}In_{0.03125}$.

From Figs. 4 and 5, we can see that the Fermi levels of both $Zn_{0.96875}In_{0.03125}O$ and $Zn_{0.9583}In_{0.0417}O$ shift upward into the CB, which shows that both of them are high doping n-type degenerate semiconductors. This accords with the analysis in Subsection 3.2. Comparing Fig. 4 and Fig. 5, we can see that the degree of the Fermi surface shifting upward into the CB varies with the doping concentration of In, which indicates that the relative electron number shifting upward into the CB changes with the doping concentration of In in ZnO. To distinguish them easily, here we let n_1 be the relative electron number shifting upward into the CB in $Zn_{0.96875}In_{0.03125}O$, and n_2 be the relative electron number shifting upward into the CB in $Zn_{0.9583}In_{0.0417}O$. From Figs. 4 and 5, we can see clearly that n_1 is determined by the area under a curve of the DOS of $Zn_{0.96875}In_{0.03125}O$ versus energy, between the bottom of the CB and the Fermi level, and n_2 is determined by the area under a curve of the DOS of $Zn_{0.9583}In_{0.0417}O$ versus energy, between the bottom of the CB and the Fermi level. $n_1 = 0.46728$ and $n_2 = 0.96764$ are obtained by integrating based on OriginPro7.5 as shown in Fig. 6. It is clearly seen that in the range of high doping concentration, the higher the doping concentration of In, the more the relative electron number shifting upward into the CB in ZnO will be.

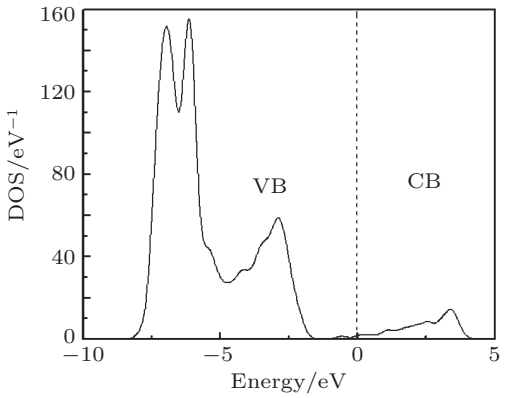


Fig. 5. Total density of states (DOS) of $Zn_{0.9583}In_{0.0417}$.

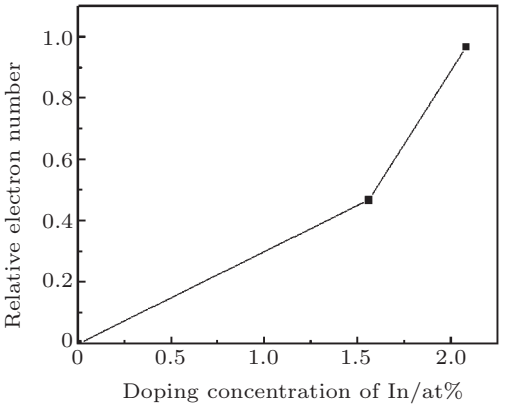


Fig. 6. Dependence of the relative electron number on the doping concentration of In.

3.3.2. Mobility

First-principles calculation in CASTEP code is based on $T = 0$ K,[23] and at this time the scattering by ionized impurities dominates in doped semiconductor. Scattering by ionized impurities is related to the doping concentration. The higher the doping concentration, the higher the scattering probability of electron by the ionized impurities in doped semiconductor is. Let N_i be the doping concentration, P_i be the scattering probability of electron by the ionized impurities, and T be the thermodynamic temperature and they are related by

$$P_i \propto N_i T^{-3/2}. \tag{1}$$

Again, the relaxation time τ_i is inversely proportional to P_i, so we have

$$\tau_i \propto N_i^{-1} T^{3/2}. \tag{2}$$

We also know that the electron mobility μ_i is

$$\mu_i = \frac{q\tau_i}{m_e^*}, \tag{3}$$

where q is the electron charge, and m_e^* is the electron effective mass.

From Eqs. (2) and (3), we can see that in the range of high doping concentration, the electron mobility μ_i is inversely proportional to the doping concentration N_i in doped semiconductor.

To quantitatively analyze the effect of high In doping on the electron mobility of ZnO, we further investigate the electron effective mass. Figiures 7–9 show that the band structures of pure ZnO, $Zn_{0.96875}In_{0.03125}O$, and $Zn_{0.9583}In_{0.0417}O$ respectively. As shown in Fig. 7, the calculated bandgap (E_g) of pure ZnO is 0.735 eV, which is close to the earlier calculated values in Refs. [12] and [24]. However, it is less than the experimental value of 3.37 eV due to the limitation of DFT in GGA, and the discontinuity in the exchange–correlation potential is not taken into account in the framework of DFT.[25]

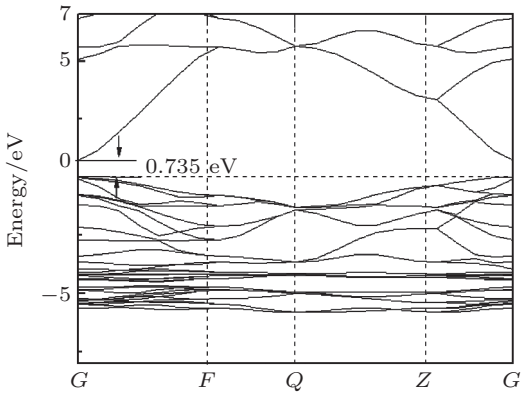


Fig. 7. Band structure of pure ZnO.

From Figs. 8 and 9, we can see that the higher the doping concentration of In, the wider the minimum band gap in ZnO is. Because the electron effective mass is proportional to the band gap width, in the range of high doping concentration, the higher the doping concentration of In, the larger the electron effective mass in ZnO is. The electron effective mass m_e^* can be expressed by the following equation:

$$m_e^* = \frac{h^2}{4\pi^2}\left(\frac{d^2E}{dk^2}\right)^{-1}, \tag{4}$$

where h is the Planck constant, E the energy, and κ the wave vector.

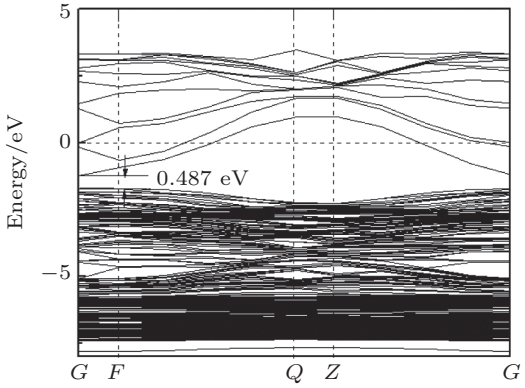


Fig. 8. Band structure (BS) of $Zn_{0.96875}In_{0.03125}O$.

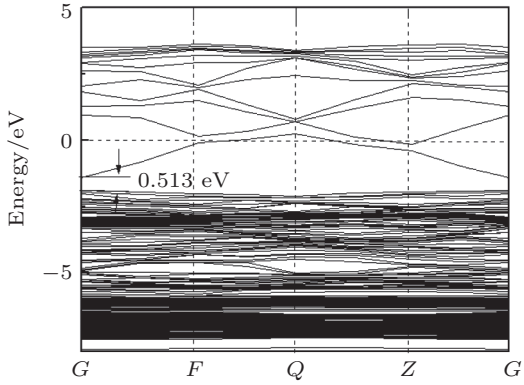


Fig. 9. Band structure (BS) of $Zn_{0.9583}In_{0.0417}O$.

Let m_{e1}^* be the electron effective mass corresponding to the G point in Fig. 8, and m_{e2}^* the electron effective mass corresponding to the G point in Fig. 9. In terms of OriginPro7.5, we obtain the second-order derivatives in the G direction of the curves at the bottom of the CB in Figs. 8 and 9. Substituting these back into Eq. (4), we have

$$m_{e1}^* = 1.724 \times 10^{-30}\ \text{kg}, \quad m_{e2}^* = 1.797 \times 10^{-30}\ \text{kg}.$$

Thus,

$$m_{e1}^* < m_{e2}^*.$$

The calculation results show that in the range of high doping concentration, the higher the doping concentration of In, the larger the electron effective mass in ZnO is, which is consistent with the above qualitative analysis results.

Now let μ_1 be the electron mobility in $Zn_{0.96875}In_{0.03125}O$, and μ_2 the electron mobility in $Zn_{0.9583}In_{0.0417}O$. From Eq. (3) we have

$$\frac{\mu_1}{\mu_2} = \frac{q\tau_1/m_{e1}^*}{q\tau_2/m_{e2}^*} = \frac{64 \times 1.797 \times 10^{-30}}{48 \times 1.724 \times 10^{-30}} \approx 1.386.$$

Thus,

$$\mu_1 > \mu_2.$$

The calculation results show that in the range of high doping concentration, the doping concentration has a greater influence on the scattering by ionized impurities than on the electron effective mass. So the higher the doping concentration of In, the lower the electron mobility in ZnO is.

3.3.3. Conductivity

In low temperature environment, the Coulomb field is formed around In^{3+} in In-doped ZnO. Under the action of the Coulomb field, the electron is scattered, and thus the resistance is generated in highly In-doped ZnO. The electron conductivity σ_i can be represented by the following equation:

$$\sigma_i = \frac{n_i q^2 \tau_i}{m_e^*} = n_i q \mu_i, \tag{5}$$

where n_i is the relative electron number shifting upward into the CB, and q the electron charge, and m_e^* the electron effective mass.

Let σ_1 be the electron conductivity in $Zn_{0.96875}In_{0.03125}O$, and σ_2 the electron conductivity in $Zn_{0.9583}In_{0.0417}O$. According to the above analysis on the relative electron number and the electron mobility, by using of Eq. (5), we have

$$\frac{\sigma_1}{\sigma_2} = \frac{n_1 q \mu_1}{n_2 q \mu_2} = \frac{0.46728 \times 64 \times 1.797 \times 10^{-30}}{0.96764 \times 48 \times 1.724 \times 10^{-30}} \approx 2.87.$$

Thus,

$$\sigma_1 > \sigma_2.$$

The calculation results show that in the range of 1 at%–2.15 at% (2.79 wt%–6 wt%) doping concentration, the conductivity decreases with the increase of the doping concentration of In in ZnO, which is consistent with the change trend of the experimental results.[17] So the experimental result in Ref. [16] is not absolutely right.

4. Conclusions

Doping concentration has a great influence on the conductivity of ZnO. Using first-principles plane-wave ultrasoft pseudopotential method based on the density functional theory (DFT), the models of the unit cell of pure ZnO, $Zn_{0.96875}In_{0.03125}O$ and $Zn_{0.9583}In_{0.0417}O$ are constructed, and the geometry optimizations of the three models are carried out. The DOS and the BS are also calculated. The calculation results show that in the range of 1 at%–2.15 at% (2.79 wt%–6 wt%) doping concentration, with the increase of doping concentration of In, the relative electron number shifts upward into the CB and electron effective mass increases, the electron mobility decreases, and also the conductivity decreases in ZnO. These are consistent with the change trend of the experimental results.[17]

Acknowledgment

Calculations were carried out at the Network Information and Computing Center of Beijing University of Aeronautics and Astronautics.

References

[1] Badeker K 1907 *Ann. Phys.* (LeiPzig) **22** 749
[2] Hong C S, Park H H, Moon J and Park H H 2006 *Thin Solid Films* **515** 957
[3] Zhou J, Fei P, Gu Y D, Mai W J, Gao Y F, Yang R S, Bao G and Wang Z L 2008 *Nano Lett.* **8** 3973
[4] Yoshino Y, Makino T, Katayama Y and Hata T 2000 *Vacuum* **59** 538
[5] Minami T, Nanto H and Takata S 1984 *Jpn. J. Appl. Phys.* **23** 280
[6] Sedky A and El-Suheel E 2012 *Chin. Phys. B* **21** 116103
[7] Gong J F, Dou Z M, Wang Z Q, Zhang B, Zhu W H, Zhang K X, Liu M Y, Zhu H and Zhou J F 2012 *Chin. Phys. B* **21** 068101
[8] Tominaga K, Takao T, Fukushima A, Moriga T and Nakabayashi I 2002 *Vacuum* **66** 505
[9] Bae S Y, Na C W, Kang J H and Park J 2005 *J. Phys. Chem. B* **109** 2526
[10] Jie J S, Wang G Z, Han X H, Yu Q X, Liao Y, Li G P and Hou J G 2004 *Chem. Phys. Lett.* **387** 466
[11] Huang Y H, Zhang Y, Gu Y S, Bai X D, Qi J J, Liao Q L and Liu J 2007 *J. Phys. Chem. C* **111** 9039
[12] Xie F W, Li P, Zhang L Q, Zhang X L, Wang X L, Wang H and Song X F 2011 *Adv. Mater. Res.* **335–336** 32
[13] Zhou X H, Hu Q H and Fu Y 2008 *J. Appl. Phys.* **104** 063703
[14] Kim K J and Park Y R 2001 *Appl. Phys. Lett.* **78** 475
[15] Li P, Deng S H, Zhang L, Zhang L, Yu J Y and Liu G H 2010 *Chin. Phys. B* **19** 117102
[16] Ye Z Z and Tang J F 1989 *Appl. Opt.* **28** 2817
[17] Lee J H and Park B O 2003 *Thin Solid Films* **426** 94
[18] Liu Q, Cheng X L, Yang X D and Fan Y H 2009 *Acta Phys. Sin.* **58** 2684 (in Chinese)
[19] Park K C, Ma D Y and Kim K H 1997 *Thin Solid Films* **305** 201
[20] Sorescu M, Diamandescu L and Tarabsanu-Mihaila D 2004 *J. Mater. Sci.* **39** 675
[21] Hou Q Y, Zhao C W and Jin Y J 2009 *Acta Phys. Sin.* **58** 7136 (in Chinese)
[22] Hou Q Y, Li J J, Zhao C W, Ying C and Zhang Y 2011 *Physica B* **406** 1956
[23] Xin J, Zheng Y Q and Shi E W 2007 *J. Inorg. Mater.* **22** 193
[24] Schleife A, Fuchs F and Furthmüller J 2006 *Phys. Rev. B* **73** 245212
[25] Anisimov V I, Aryasetiawan F and Lichtenstein A I 1997 *J. Phys: Condens. Matter* **9** 767